Chapter

New Landmarks, Signs, and Findings in Optical Coherence Tomography

Francisco Javier Lara-Medina, Olivia Esteban, Isabel Bartolomé, C. Ispa, Javier Mateo and Francisco Javier Ascaso

Abstract

Spectral domain optical coherence tomography (SD-OCT) is a common useful noninvasive imaging instrument which is used for the diagnosis and follow-up of macular disorders. The clinical findings by OCT in these pathologies are well known. Currently, due to the development of this technology and its wide use, new OCT findings have been reported in the literature. The aim of this chapter is to describe new pathological or abnormal signs and findings in SD-OCT, including hyperreflective spots or dots, flyer saucer sign, outer retinal tubulations, dipping sign, focal choroidal excavation, outer retina-choroid complex splitting, foveal pseudocyst, brush border pattern, dome-shaped macula, pearl necklace sign, choroidal macrovessel, cystoid foveal degeneration, and disorganization of the retinal inner layers (DRIL).

Keywords: hyperreflective spots, perifoveal cupping, flyer saucer sign, tubulations, dipping sign, outer retina-choroid complex splitting, foveal pseudocyst, brush border pattern, dome-shaped macula, pearl necklace sign, macrovessel, disorganization of the retinal inner layers

1. Introduction

Spectral domain optical coherence tomography (SD-OCT) is a common useful noninvasive imaging instrument which is used for the diagnosis and follow-up of macular diseases, such as age-related macular degeneration (AMD), diabetic macular edema (DME), epiretinal membrane (ERM), or macular hole. The clinical findings by OCT in these pathologies are well known. SD-OCT allows detail assessment of the retinal thickness and morphologic evaluation of the retinal layers. Currently, due to the development of this technology and its extensive use, new OCT findings have been reported in the literature. The higher resolution and speed of SD-OCT have improved the accuracy and reproducibility of macular imaging and have allowed an enhanced assessment of the integrity of the outer retinal bands.

2. New landmarks in OCT

OCT imaging is similar to ultrasonography, except that it uses infrared light reflections instead of acoustic waves. The OCT image is displayed using a false color map that corresponds to detected backscattered light levels from the incident light. White and red colors represent high reflectivity signals, while the low reflectivity signals correspond to black and blue colors [1]. OCT interpretations make necessary knowledge of the normal anatomy of the retina. In a usual SD-OCT scan, a highly scattering layer delineates the posterior boundary of the retina and corresponds to the retinal pigment epithelium (RPE) and choriocapillaris complex. The nerve fiber layer is manifest as a highly backscattering red layer at the vitreoretinal interface. Both layers are the posterior and anterior boundaries of the sensory retina and are essential to quantify the neurosensorial retinal thickness [2]. The rest of the layers of the neurosensorial retina are disposed between the two limits, and they are observed with OCT in a similar way to a histological section. The high reflectivity signal (yellow and red colors) come from the retinal nerve fiber layer (RNFL), inner plexiform layer, outer plexiform layer (OPL), internal limiting membrane (ILM), junction between inner and outer segments of photoreceptors (IS/OS), and RPE and choriocapillaris complex. The low reflectivity signals (black and blue colors) correspond to the nuclear layers [3]. In 2014, an international panel of OCT experts agreed on the adequate nomenclature for the retinal layers as visualized on OCT [4]. The new terminology of the outer retinal bands and their anatomical correspondence are described below, from the innermost to the outermost (**Figure 1**) [4, 5]:

1. The external limiting membrane band (ELM) is located at the boundary between the nuclei (cell bodies) and the inner segments of the photoreceptors and comprises clusters of junctional complexes between the Müller cells and the photoreceptors.

2. The ellipsoid zone (EZ), which was previously referred as the photoreceptor inner segment/outer segment (IS/OS) junction, is considered to be formed mainly by mitochondria within the ellipsoid layer of the outer portion of the inner segments of the photoreceptors. In a normal fovea, the distance from the EZ line to the ELM line is shorter than that from the EZ line to the RPE. The EZ "elevation" in the foveal center is due to elongated foveal cone outer segments.

3. The interdigitation zone (IZ) is considered to be the contact cylinders formed by the apices of the RPE cells that encase the part of the cone outer segments. This layer is not always recognizable from the underlying RPE layer, even in healthy subjects.

4. The retinal pigment epithelial band is formed by the RPE and Bruch's membrane. Both structures are indistinguishable from each other using the currently commercial SD-OCT. In the fovea, this band is thicker compared to other regions, which indicates that choroidal structures may also participate in the hyperreflectivity of the RPE band at this location.

Recent publications have reported that the damage or the alteration of the photoreceptors supposes a loss of integrity of some of these four bands previously described [6, 7]. Series of OCT images in different phases of degenerative diseases of the retina have demonstrated that IZ, EZ, and ELM lengths are highly correlated with each other. The affectation seems to occur in a stepwise sequence: first at the

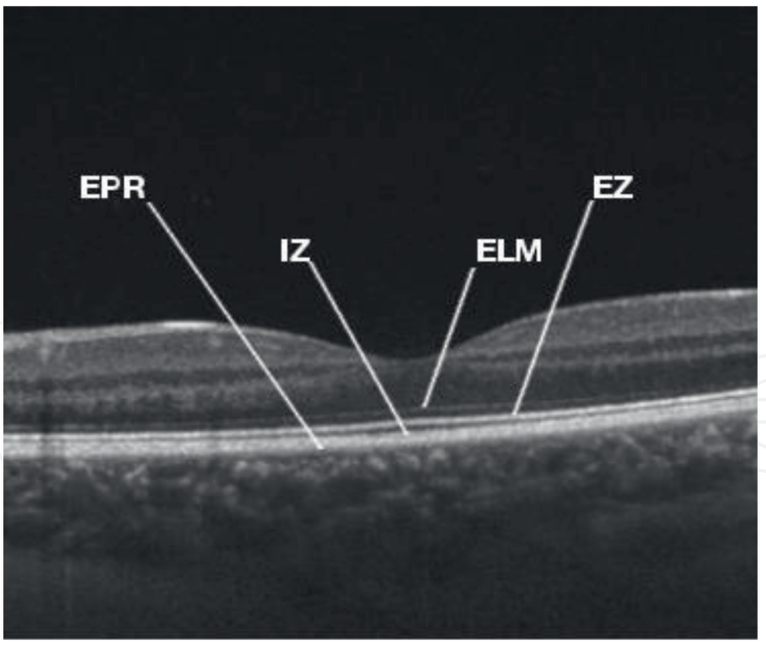

Figure 1.
Spectral domain optical coherence tomography (SD-OCT) scan with external retinal landmarks from a healthy subject. RPE: retina pigment epithelium; IZ: interdigitation zone; EZ: ellipsoid zone; and ELM: external limiting membrane.

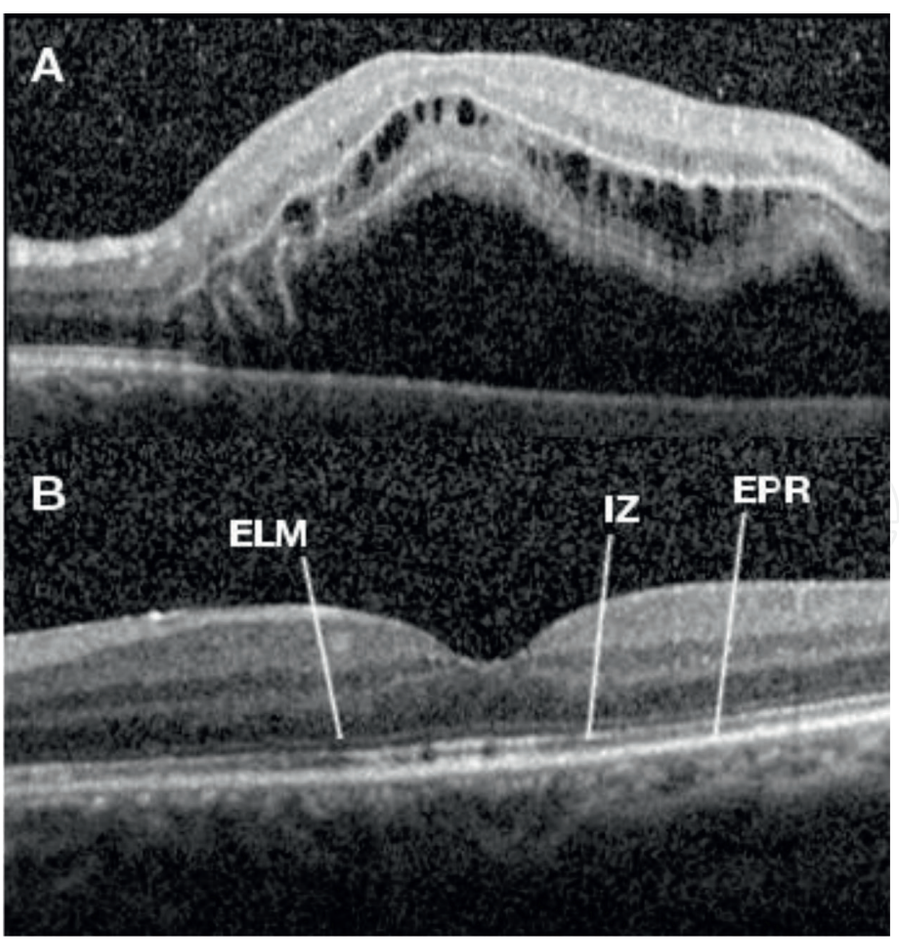

Figure 2.
SD-OCT in a patient with retinal detachment macula off (A). Post-surgical aspect through OCT of the same patient in which the integrity of the outer layers is observed (B). The visual acuity was 20/30.

IZ, followed by the EZ, and finally the ELM band [7–9]. Similarly, photoreceptor restoration seems to occur in the reverse order. After closing a macular hole, it has been documented that the ELM zone is the first structure to recover, and its recovery has been considered a sign of intact Müller cells and photoreceptor cell bodies [10]. Also, OCT findings after ERM and macular hole surgeries showed that recovery of EZ line only occurred in areas with intact ELM, and IZ recovery was only observed in eyes with EZ and ELM uninjured [11, 12]. The recovery of the ELM line following treatment has been correlated with visual acuity outcomes for macular hole [11, 13], retinal detachment [9], and AMD [14]. After macular hole closure, the presence of injured ELM was associated with reduced visual acuity [12]. In retinal detachment (RD), preservation of the ELM line postoperatively was related with better visual acuity result and also seems to predict the subsequent restoration of the photoreceptor layer [9]. Disruption or absence of the EZ line has been shown to correlate with visual acuity and severity in several retinal diseases [5]. In non-neovascular AMD, disruption of the EZ has been associated with visual impairment [15–17]. Furthermore, retinal sensitivity in patients with geographic atrophy was significantly higher in areas with an uninjured EZ [18]. In neovascular AMD, intact EZ at baseline was reported as a favorable prognostic factor for visual acuity outcome following intravitreal anti-vascular endothelium growth factor (anti-VEGF) treatment [14]. In diabetic patients with macular edema, the EZ disruption at the fovea was reported as a significant predictor of visual acuity [19, 20]. In eyes with ERM, preoperative disruptions of the EZ line were also associated with poorer visual acuity outcomes [21–23]. The IZ line is very difficult to identify even in healthy subjects. A correlation between the postoperative status of IZ and visual acuity has been described for macular hole [11], ERM [21], and RD [24]. Gharbiya and collaborators reported that the integrity of the IZ line was the strongest predictor of visual acuity outcome after primary RD repair (**Figure 2**) [24]. Following macular hole surgery, patients with irregular or discrete IZ line had significantly better visual acuity compared with those eyes with a disrupted or absent IZ line at the one-year visit follow-up [14]. In recent years, new OCT findings and signs have been reported for different retinal diseases. We will describe them with more clinical relevance.

3. New findings and signs

3.1 Hyperreflective retinal spots (HRS)

Coscas and cols were the first authors to report the presence of HRS on SD-OCT in exudative AMD [25]. These dots are described as small in size (20–40 μm in diameter), punctiform hyperreflective elements (equal or higher reflectivity than the RPE band), distributed throughout all retinal layers. HRS are mainly located at the border of the ONL and within the OPL [26]. They have also been reported in early stages of DR and also in diabetics without any clinical sign of DR, DME, retinal venous occlusion (RVO), central serous chorioretinopathy (CSCR), macular telangiectasias, and certain types of uveitis (**Figure 3**) [27]. It has been hypothesized that HRS represent aggregates of microglial activated cells and could indicate a retinal inflammatory response. Therefore, it has been reported reduction of HRS number following intravitreal anti-VEGF or dexamethasone therapies [28]. There are various theories on the pathogenesis of HRS. Some authors hypothesize that HRS are focal pigment accumulations of lipofuscin granules. Others consider that there could be small intraretinal protein or lipid deposits/exudates secondary to the breakdown of the blood-retinal barrier in retinal vascular diseases [26–30]. According to other theory, HRS might be derived from the degenerated photoreceptors or from the macrophages that

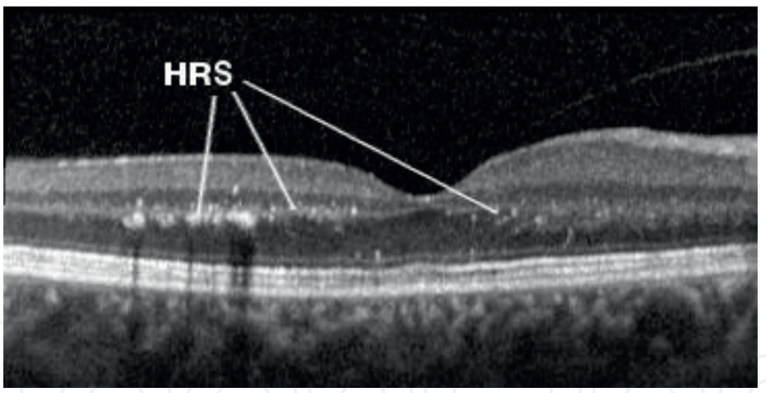

Figure 3.
Hyperreflective retinal spots (HRS) observed in a patient affected of tuberculosis posterior uveitis.

phagocyted them [31]. Concerning the clinical implications of the HRS, we have already commented that they represent a certain degree of retinal inflammation. HRS are associated with poorer visual outcome in patients with macular edema due to retinal vascular diseases such as RD or RVO. The therapeutic response to specific treatments might be different according to the number of HRS. Hwang et al. reported an inadequate response to intravitreal bevacizumab for DME and macular edema due to RVO in eyes with a greater number of HRS. Eyes that responded poorly to bevacizumab were treated with dexamethasone implants. About 75% of such eyes showed a good response and corresponded to the eyes with a higher number of HRS [32]. Vujosevic and cols have also suggested that DME with a high number of HRS and a large area of increased foveal autofluorescence showed better morphologic and functional results (better retinal sensitivity) if, at least initially, was treated with intravitreal steroids versus anti-VEGF [28]. These findings suggest that in eyes with several HRS, the inflammatory pathway might contribute to the pathogenesis of the macular edema more than the VEGF pathway. Therefore, in patients with macular edema and many HRS, anti-inflammatory drugs (e.g., dexamethasone intravitreal implant) might be more effective than intravitreal anti-VEGF treatment [32].

3.2 Flying saucer sign

The use of hydroxychloroquine (HCQ), an antimalarial drug utilized for a range of rheumatologic and dermatologic diseases, is associated with a low incidence of retinopathy (1% after 5 years) when used at recommended doses (<6.5 mg/kg/day) [33]. However, the retinopathy described as a bull's-eye is untreatable and tends to progress even after cessation of the drug. In recent years, there is an increased interest in screening by using multimodal imaging techniques to detect early signs of retinal toxicity. SD-OCT may detect significant structural alterations before the development of visible HCQ retinopathy. Several OCT findings have been described in the literature such as disruption of the EZ line, loss of the ELM, parafoveal thinning of the ONL, and RPE damage. These studies suggest that there is a foveal resistance to HCQ damage as demonstrated by the preservation of the subfoveal outer retinal layers. This foveal sparing originates the "flying saucer" sign on HCQ retinopathy (**Figure 4**) [34]. The main characteristics of this sign include the loss of the normal foveal depression, perifoveal thinning of the ONL, an ovoid appearance of the central fovea, conservation of the outer retinal structures and photoreceptor IS/OS junction in the central fovea, an apparent posterior displacement of the inner retinal structures toward RPE, and perifoveal loss of the photoreceptor IS/OS junction [3]. All these alterations originate an ovoid appearance in the central fovea [35]. This sign is neither pathognomonic nor necessary for the diagnosis of HCQ

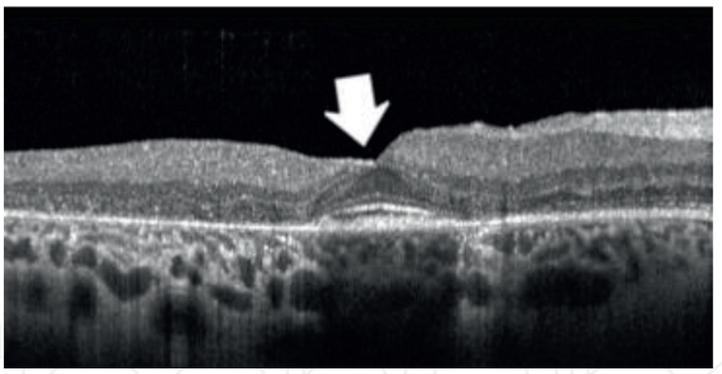

Figure 4.
SD-OCT revealed the "flying saucer" sign in a woman treated with oral chloroquine at a dosage of 3 mg/kg once daily for 8 years.

retinopathy. Nevertheless, its visualization on SD-OCT images should alert us to possible retinal toxicity due to HCQ toxicity.

3.3 Outer retinal tubulation (ORT)

ORT is a degenerative process of outer retinal reorganization located primarily in eyes where the macula is disrupted and RPE is absent. ORTs are ovoid or circular hyporeflective lesions surrounded by a hyperreflective ring always located in the ONL in eyes with advanced outer retinal diseases (**Figure 5**) [36]. It has been described in numerous retinal disorders showing macular atrophy involving RPE, such as AMD [36], mitochondrial diseases [37], and retinal dystrophies [38]. They have also been reported in cases of macular neovascularization including AMD, choroidal nevus, pseudoxanthoma elasticum [39], multifocal choroiditis with uveitis and CNMV, choroideremia [36], and enhanced S-cone syndrome [40]. Histologic studies showed interconnecting tubes of surviving cone photoreceptors interleaved with and contained by processes of Müller cells [41]. Histologically, the hyperreflective border of ORS seen in SD-OCT images corresponds with the presence of both an EML delimiting the lumen and mitochondria migrating from the inner segments to the cell bodies of degenerating cone photoreceptor. The main histologic characteristics of ORTs are [41]:

1. location at the level of ONL
2. presence of an ELM surrounding all or part of the lumen
3. presence of enclosing radially oriented photoreceptors pointing to the lumen
4. disruption or absence of the underlying RPE

There are different shapes of ORTs: open, closed, forming, and branching. A branching or pseudodendritic pattern is observed mainly in macular neovascularization, whereas a single tube is more frequent in the border of geographic atrophy [42]. Regarding the etiology of these tubulations, it has been hypothesized to be related to the different shapes of the ELM descent (flat, curved, and reflected). As the RPE begins to atrophy, the ELM descent changes from flat to curved, then reflected to scrolled, and finally, an area of ORT may appear. In this process, Müller cells expand and fill the spaces created by the loss of photoreceptors, as they are the only structure persisting in end-stage of ORT. The presence of a scrolled ELM descent may represent a predictive factor for progression toward ORT. It has been reported that in cases of neovascularization, the progression to ORT experienced a shorter period between

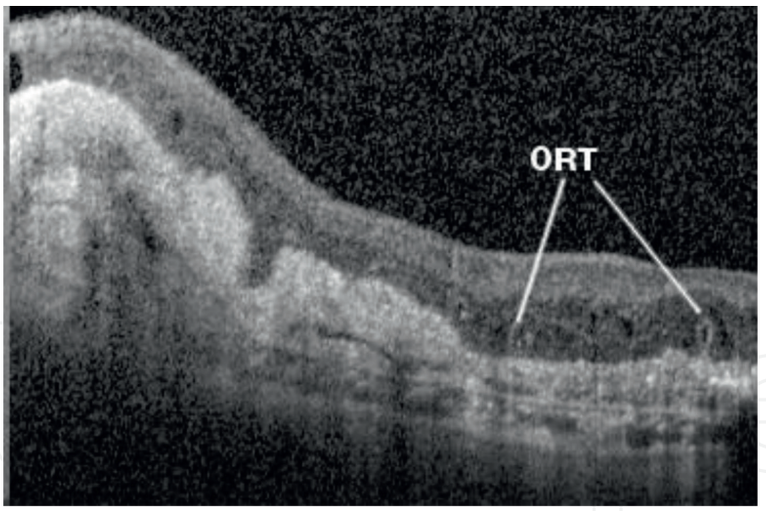

Figure 5.
Outer external tabulation in atrophic age-macular degeneration.

the steps of flat and curved ELM than eyes only with atrophic [42]. ORTs have a significant prognostic value since their presence suggests a poor visual acuity. They should be differentiated from intraretinal or subretinal fluid cysts located at the outer retinal layers. Intraretinal fluid cysts in cystoid macular edema (CME) have the arrangement as a petaloid manner, while ORTs are randomly arranged at the macula. Pseudocysts are usually distinguished from ORTs because they are located in the inner nuclear layer. Retinal tubulations are always located at the level of the ONL [3]. ORTs are circular hyporeflective lesions surrounded by a hyperreflective ring. This hyperreflective border is absent in cysts. Likewise, ORTs may contain a few focal hyperreflective spots in contrast to the completely hyporeflective cystoid lesions. The recognition of ORT may avoid unnecessary treatment because it is more refractory to anti-VEGF treatment compared to the cysts. Because outer tubulations tend to change slowly over time, it is unlikely to be associated with an active exudative or inflammatory process. For that reason, they do not require treatment [3, 42]. ORT can also be differentiated from rosettes described in retinoblastoma by their large size, tubular structure, and degenerative instead of developmental nature. In retinitis pigmentosa, there are also rosettes which are distinguished from ORTs by their location outside the macula and absence of degeneration of the underlying RPE [42].

3.4 Dome-shaped macula

Dome-shaped macula (DSM) is an inward protrusion of the macula as visualized by OCT (**Figure 6**). Different patterns have been described by OCT: a horizontal or vertical oval-shaped dome and a round dome [43]. DSM was first reported in myopic eyes with posterior staphyloma, but more recently has also been described

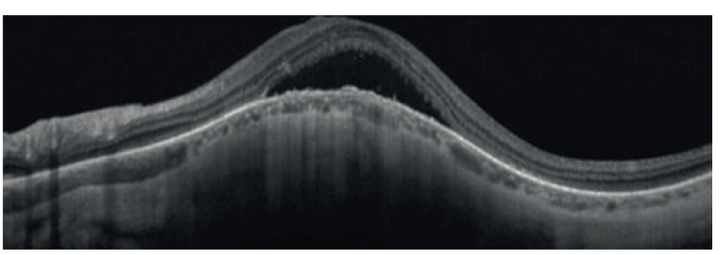

Figure 6.
SD-OCT showing a dome-shaped macula.

in patients without staphyloma, emmetropic, or hypermetropic eyes [44, 45]. A variety of hypotheses have been postulated to explain it: an adaptive mechanism to minimize defocus in highly myopic eyes [46], vitreomacular traction [47], ocular hypotony [47], resistance of the sclera to the staphylomatous deformation [48], or localized choroidal thickening [48]. However, it has been recently indicated that the main problem is the different degrees of scleral thinning in the foveal region [46, 49, 50]. Subretinal fluid (SRF) in the fovea has been associated continuously with DSM in 28.5–66.6% of patients [51]. It may be due to RPE dysfunction [48] or as a consequence of not uniform scleral thickness that can affect choroidal fluid [46]. Although photodynamic therapy and anti-VEGF agents have been applied, they had no effects in terms of improvement in BCVA and resolution of SRF, because the fluid remained chronic and stable in most of the eyes over time [51], and it was even spontaneously resolved in 47% of the cases [52].

3.5 Brush border pattern or elongation of photoreceptor outer segment

Brush border pattern is defined as an accumulation of waste products in the photoreceptor outer segment on the outer surface of the detached neurosensory retina over subretinal fluid (**Figure 7**). This provides an irregular, serrated, and thicker appearance of the detached neurosensory retina. Other authors denominate it as "elongation of the outer photoreceptor segment", and it can be found in almost 73–75% of OCT images from patients who suffer CSCR [53]. The loss of the contact between RPE and photoreceptor outer segments that occur in CSCR prevents the waste product of photoreceptors being phagocytosed by RPE [54]. These subretinal proteins or accumulated macrophages with outer photoreceptor segments can be observed as hyperfluorescent white-yellowish precipitates in the retinal examination if they contain precursors of lipofuscin [55]. If this process persists, despite subretinal fluid absorption, subretinal deposits may progress to be permanent with the subsequent poor visual outcome. Complete disappearance of outer segments as observed in very long-standing CSCR correlates with poor visual prognosis [53].

3.6 Outer retina-choroid complex (ORCC) splitting

Patients at intermediate clinical stages in Best vitelliform macular dystrophy (BVMD) show split in the ORCC by OCT. The ORCC has multiple components, and it is split into subcomponents showing different patterns [56]. Such patterns of ORCC splitting represent the separation between the apical surface of the RPE and photoreceptors causing neurosensory macular retinal detachment (**Figure 8**) [57]. OCT shows a diffuse, irregular, and thickened ORCC by underlying hyporeflective area [3].

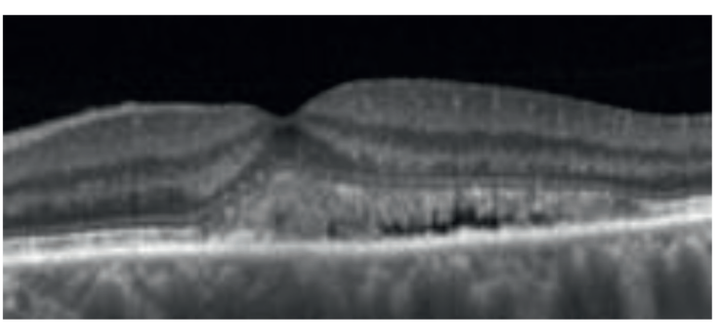

Figure 7.
Brush border pattern in patient affected of chronic central serous chorioretinopathy (CSCR).

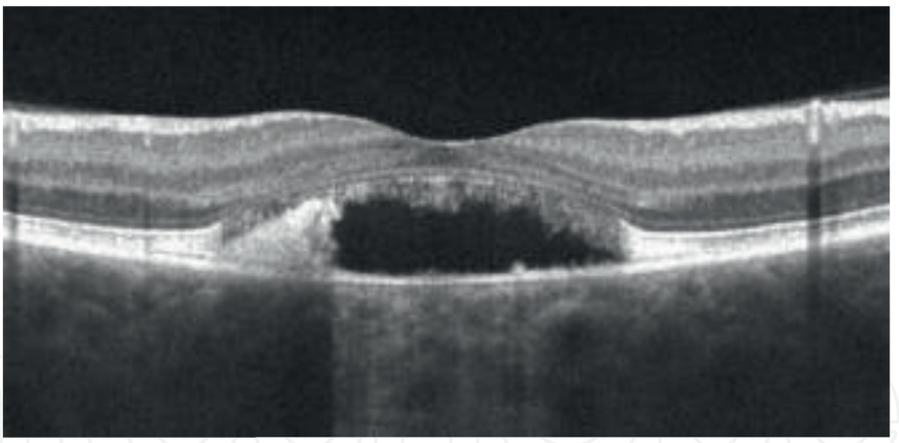

Figure 8.
SD-OCT shows a splitting of outer retina-choroid complex by hyporeflective area in a patient with Best vitelliform macular dystrophy.

3.7 Disorganization of retinal inner layers (DRIL)

DRIL is observed on OCT as the difficulty to identify limits between the ganglion cell-inner plexiform layer complex, inner nuclear layer, and OPL (**Figure 9**). It represents an interrupted transmission pathway between the photoreceptors and ganglion cells due to the disruptions of synaptic connections of amacrine, bipolar, and horizontal cells [58]. Several hypotheses explain the pathogenesis: **mechanical factor** (stretching of bipolar axons by edema) and **vascular factors** (ischemia, loss of the retinal capillary plexuses, or neuroglial degeneration as sequelae of inflammation) [58–62]. DRIL has been described as a strong predictive factor of worse visual acuity in patients with DME [58], uveitic macular edema [63], and central retinal vein occlusion [64]. Although the role of ischemia in DRIL is being studied, authors have found that areas of macular capillary nonperfusion were strongly correlated with DRIL on fluorescein angiography (FA) in severe nonproliferative and proliferative diabetic retinopathy (PDR) [59]. Moreover, more recently, OCT angiography has allowed researchers to study the positive correlation between DRIL and the size of the foveal avascular zone in diabetic retinopathy and retinal vein occlusion [60, 65]. Even, it has been associated with higher body mass index, longer diabetes duration, and increasing severity of PDR [66, 67]. Several studies have demonstrated that DRIL is a dynamic phenomenon. Its reversibility, with an anatomic improvement, decreases with increasing duration [58, 68]. Thus, DRIL seems to be a biomarker that may be incorporated into daily clinical practice and be a useful tool in the future therapeutic intervention [69].

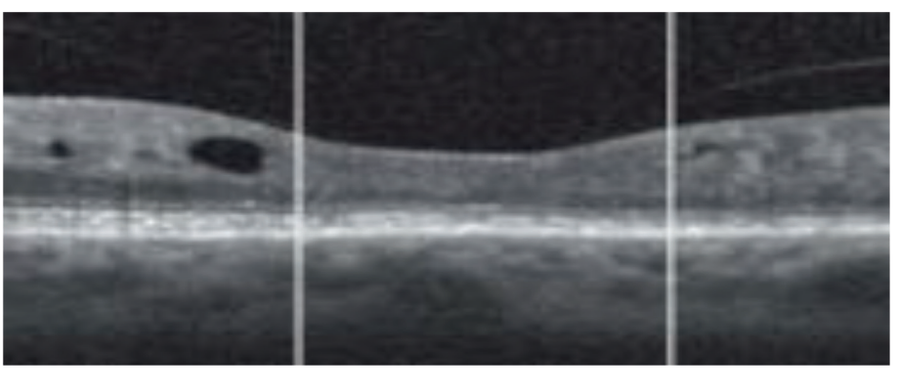

Figure 9.
DRIL areas in SD-OCT.

3.8 Pearl necklace sign

The pearl necklace sign refers to HRD in a continuous ring around the cystoid spaces in the retina that has been seen in diseases with exudative maculopathy, vascular leakage, and chronic CME such as neovascular AMD, DME, retinal vein occlusion, retinal arterial macroaneurysm, or Coats disease (**Figure 10**) [70]. The authors speculated that HRD indicated the presence of lipid material from retinal vascular leakage similar to hard exudates. These pearls may represent lipid-filled macrophages along the inner wall of retinal edema [70]. Moreover, it is considered a frequent precursor sign on the location of the hard exudates which appear later. Therefore, this sign can change shape and may resolve under treatment or spontaneously. The presence of pearl necklace sign has not been associated with worse visual acuity in RD [71].

The pearl necklace sign should be differentiated from ORTs, which are located deeper in the ONL of the retina. In ORT, the ring is continuous and homogeneous, whereas the hyperreflective ring is as small foci in the pearl necklace sign [3].

3.9 Focal choroidal excavation (FCE)

FCE is a localized depression of the choroid detected only by using OCT, without any evidence of posterior staphyloma or scleral ectasia. It affects Bruch's membrane-RPE-choriocapillaris line complex line and photoreceptors (**Figure 11**). Patients are mostly asymptomatic and have good visual acuity. Nevertheless, some lesions may be associated with the development of choroidal neovascular membrane. It has been reported that FCE may appear in certain macular disorders such as CSCR, AMD, ERM, CNVM, polypoidal choroidal vasculopathy, BVMD, Vogt-Koyanagi-Harada disease, punctate inner choroidopathy, focal retinochoroiditis, foveoschisis, torpedo maculopathy, multiple evanescent white dot syndrome, multifocal choroiditis, and combined hamartoma of the retina and RPE [3]. OCT allows to identify retinal and choroidal structures that are affected in the excavation, which usually includes RPE, Bruch's membrane, EZ line, ELM, and ONL which followed the contour of the FCE. In some cases, it can be appreciated an attenuation or absence of IS/OS junction at the excavation, and ONL was thickened in most conforming eyes [72]. However, the layers from the OPL to the ILM were undisturbed, and also the sclerochoroidal junction appeared reasonably preserved without scleral excavation [72, 73]. FCE may be organized in two patterns, whether or not the photoreceptor layer is detached

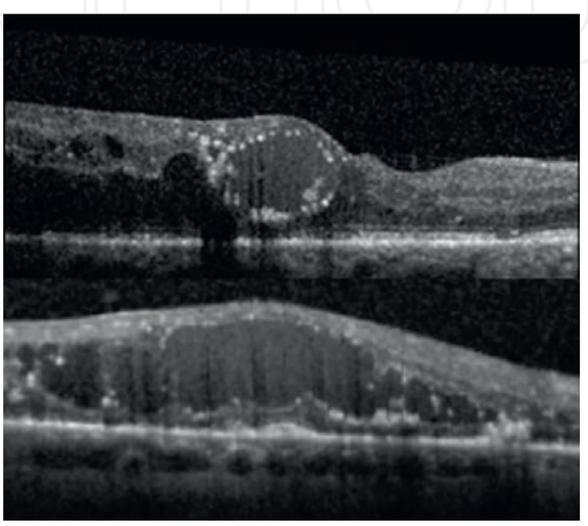

Figure 10.
Pearl necklace sign in patients with severe diabetic macular edema.

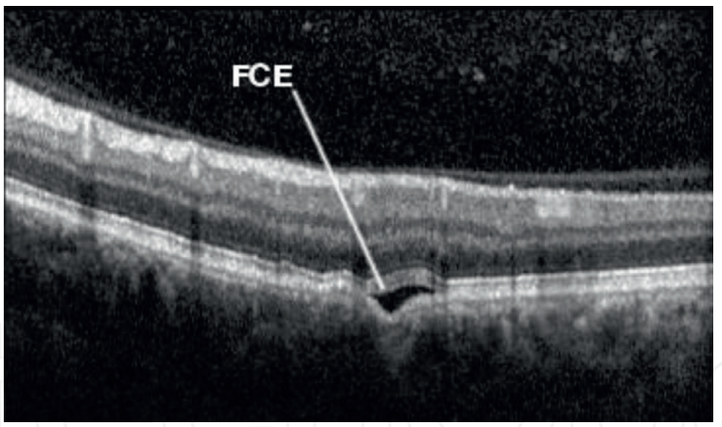

Figure 11.
Focal choroidal excavation (FCE) revealed by SD-OCT in a patient with chronic CSCR and systemic lupus erythematosus.

from the RPE. Thus, conforming FCE describes those types of lesions without separation between the two layers and the photoreceptors adapt to the contour of the RPE layer. On the other hand, in nonconforming FCE, photoreceptors appeared to be detached from the RPE showing a hyporeflective space. Factors contributing to the formation of each pattern are unknown [74]. Other authors have classified the lesions into three morphological patterns based on SD-OCT findings: bowl shaped, cone shaped, and mixed shaped [75]. They observed that all bowl-shaped types showed atrophic changes and RPE irregularities, whereas in cone-shaped FCE, a less atrophic change is detected at the center of the lesion. The pathogenesis of FCE is still unknown. Some authors suggest it could be related to a congenital defect within the choroid, which is supported by the fact that shape and size remained stable during the follow-up in most of the reported cases [73]. Nevertheless, no family history and low prevalence in young people suggest that it may be an acquired condition [74]. Some authors proposed FCE is an entity related to inflammatory diseases like Vogt-Koyanagi-Harada disease, multiple evanescent white dot syndrome, and other types of retinochoroiditis [76].

3.10 Foveal pseudocyst

Foveal pseudocyst is an OCT pathologic sign that is caused by subretinal retention of perfluorocarbon liquid (PFCL) after vitreoretinal surgery. Subretinal PFCL is a serious complication if it affects fovea. The incidence ranges from 1 to 11% after retinal detachment surgery [77]. Main risk factors for this entity are the presence of a large size retinal tear, large retinotomy (especially in 360°), and retinal traction at retinal breaks [78]. It is rare to find it in conventional surgery, but in these cases, it is usually caused by small bubbles which can be produced by turbulence by the interface between PFCL and saline solution [77]. OCT is a useful tool to identify intraretinal bubbles of PFCL. In many cases, the bubbles remain stable without size changing. The most common signs in OCT are RPE pigment disorganization, disruption of ellipsoid layer, and hyperreflectivity at the base of the PFCL bubble (**Figure 12**) [77]. It has been reported several cases with retinal hole secondary to long-standing subretinal PFCL [79]. Subretinal PFCL is responsible for retinal damage resulting in loss of visual acuity, scotomas, and retinal thinning. Long-time exposure to PFCL can lead to RPE atrophy, photoreceptor damage because there is a direct toxic defect, or inflammatory response including macrophages phagocyted PFCL [77]. It is recommended to remove PFCL bubbles located beneath the macula or if there is a tendency to move to the macular area [80].

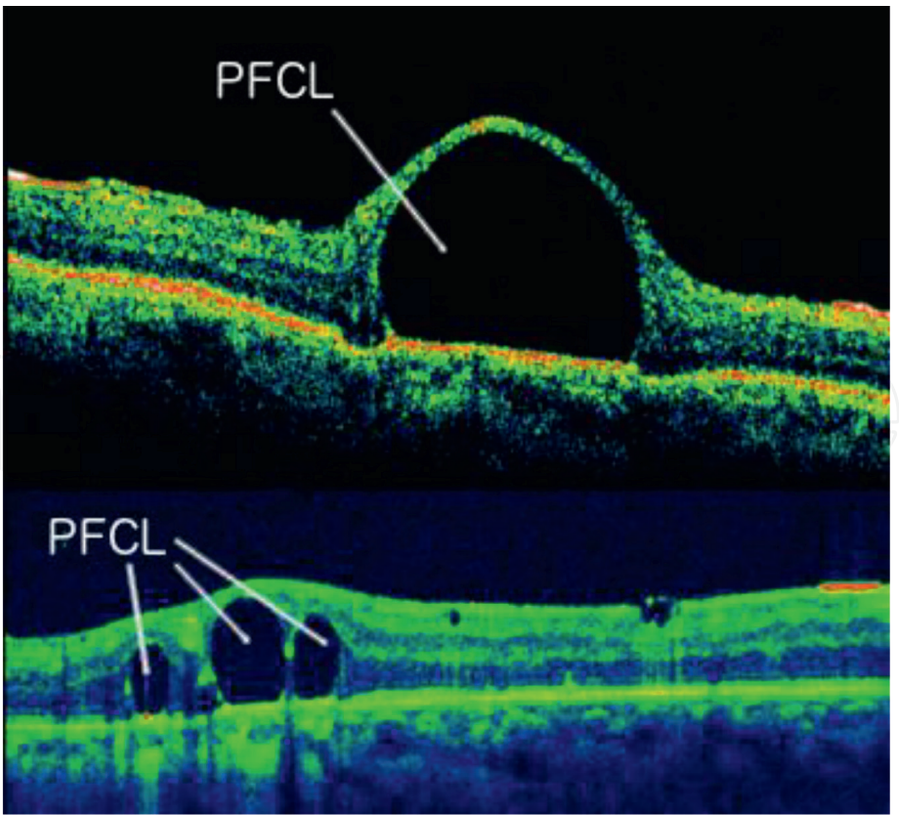

Figure 12.
Subretinal retention of perfluorocarbon liquid (PFCL) after retinal detachment surgery.

3.11 Choroidal macrovessel

It is a rare ocular lesion which appears on fundus examination as an abnormal, tortuous vessel deep to the retina. It was first described as a serpiginoid atrophic lesion in the temporal macula, with an orange-red aspect and several unspecific choroidal spots in the posterior pole [81]. Choroidal macrovessel is not associated with acute inflammation and symptoms. Some reports have shown hyperpigmentation of the RPE, debris in the subretinal space, and changes in the outer nuclear layer (ONL) thickness [82, 83]. SD-OCT reveals a tubular structure which shows hyperreflectivity band below RPE representing the superior edge of the lesion, with an elevation of RPE and photoreceptor and posterior shadowing [81]. In recent studies, it has been explored with enhanced-depth imaging spectral domain optical coherence tomography (EDI SD-OCT) showing a vascular structure that traversed the entire choroidal thickness and produces an indentation at the choroidal-scleral junction and the ellipsoid zone (EZ) causing a reduction of the ONL thickness [82, 83]. A differential diagnosis from choroidal macrovessel should be made with subretinal nematode tract, choroidal hemangioma, inflammatory choroidopathy, retinochoroidal anastomosis, vortex varix, and aberrant long posterior ciliary artery [81, 83].

3.12 Dipping sign

It is a pathologic retinal sign that may be appreciated with high-resolution OCT images in some patients with acute CSCR. It is characterized by getting an inverted triangle shape at the outer surface of the detached retina, in those eyes with fibrinous exudate in the subretinal space that protrudes over the RPE [3]. The primary cause of dipping sign seems to be traction due to the fibrinous exudates and the swelling of

the ONL. It has been reported that some of the leakage sites (20.3%) show fibrinous exudate as a highly reflective area in the subretinal space, around the leakage site [84]. Additional observations with SD-OCT include thickening of the outer photoreceptor segment layer with invisibility of the inner segment-outer segment junction line and "dipping" of the posterior retinal layer toward the RPE [84, 85]. In later stages, granular deposits may become visible at the posterior surface of the detached retina [85]. It has been documented a decrease in foveal thickness once CSCR is resolved.

3.13 Cystoid foveal degeneration (CDF)

CDF is a rare form of macular pathology that can be precisely diagnosed only with OCT. It is characterized by large cystic spaces, or in some cases, giant single cyst in the fovea. It can occur with or without thinned septa between cystic spaces. Usually, it affects patients with diabetic maculopathy, uveitis, RVO, AMD, associated with Streptococcus constellatus endocarditis, and CSR [3, 86]. The hyperreflective OCT appearance of these lesions, followed by cystic change and permanent visual loss, suggests that they might represent retinal infarctions. Their predilection for the fovea may reflect the high metabolic demand at this area of the retina and the narrow-bore capillaries of the perifoveal vasculature.

This pathology is associated with a distortion of IS/OS layer and loss of outer segment of photoreceptors. In comparison with CME, CDF has a more extensive and multitude cysts. As opposed to CME, although CDF cysts may shrink or disappear, there is a limited improvement in visual acuity [3]. FA and fundus autofluorescence (FAF) are not capable of distinguishing CME from CDF.

Acknowledgements

Thanks to Antonio Arias Palomero and José Juan Valdés González for the effort of searching some of the images showed in this chapter.

Conflicts of interest

Dr. Ascaso reports nonfinancial support from Topcon and Zeiss. All remaining authors have declared no conflicts of interest. All coauthors have seen and agreed with the contents of the manuscript.

Author details

Francisco Javier Lara-Medina[1,2*], Olivia Esteban[1,2], Isabel Bartolomé[1,2], C. Ispa[1,2], Javier Mateo[1,2] and Francisco Javier Ascaso[1,2,3]

1 Department of Ophthalmology, Hospital Clínico Universitario "Lozano Blesa", Zaragoza, Spain

2 Aragon Health Research Institute (IIS Aragon), Zaragoza, Spain

3 School of Medicine, University of Zaragoza, Zaragoza, Spain

*Address all correspondence to: javierlara@me.com

References

[1] Arevalo JF, Lasave AF, Arias J, Serrano M, Arevalo F. Clinical applications of optical coherence tomography in the posterior pole: The 2011 José Manuel Espino lecture—part I. Clinical Ophthalmology. 2013;**7**:2165-2179

[2] Chauhan DS, Antcliff RJ, Rai PA, Williamson TH, Marshall J. Papillofoveal traction in macular hole formation: The role of optical coherence tomography. Archives of Ophthalmology. 2000;**118**(1):32-38

[3] Turgut B, Demir T. The new landmarks, findings and signs in optical coherence tomography. New Frontiers in Ophthalmology. 2016;**2**(3):131-136

[4] Staurenghi G, Sadda S, Chakravarthy U, Spaide RF. Proposed lexicon for anatomic landmarks in normal posterior segment spectral-domain optical coherence tomography. Ophthalmology. 2014;**121**(8):1572-1578

[5] Saxena S, Srivastav K, Cheung CM, Ng JY, Lai TY. Photoreceptor inner segment ellipsoid band integrity on spectral domain optical coherence tomography. Clinical Ophthalmology. 2014;**8**:2507-2522

[6] Spaide RF, Curcio CA. Anatomical correlates to the bands seen in the outer retina by optical coherence tomography: Literature review and model. Retina. 2011;**31**(8):1609-1619

[7] Mitamura Y, Mitamura-Aizawa S, Katome T, Naito T, Hagiwara A, Kumagai K, et al. Photoreceptor impairment and restoration on optical coherence tomographic image. Journal of Ophthalmology. 2013;**2013**:1-7

[8] Aizawa S, Mitamura Y, Hagiwara A, Sugawara T, Yamamoto S. Changes of fundus autofluorescence, photoreceptor inner and outer segment junction line, and visual function in patients with retinitis pigmentosa: Autofluorescence in retinitis pigmentosa. Clinical & Experimental Ophthalmology. 2010;**38**(6):597-604

[9] Wakabayashi T, Oshima Y, Fujimoto H, Murakami Y, Sakaguchi H, Kusaka S, et al. Foveal microstructure and visual acuity after retinal detachment repair. Ophthalmology. 2009;**116**(3):519-528

[10] Bottoni F, De Angelis S, Luccarelli S, Cigada M, Staurenghi G. The dynamic healing process of idiopathic macular holes after surgical repair: A spectral-domain optical coherence tomography study. Investigative Ophthalmology & Visual Science. 2011;**52**(7):4439

[11] Ooka E, Mitamura Y, Baba T, Kitahashi M, Oshitari T, Yamamoto S. Foveal microstructure on spectral-domain optical coherence tomographic images and visual function after macular hole surgery. American Journal of Ophthalmology. 2011;**152**(2):283-290.e1

[12] Shimozono M, Oishi A, Hata M, Kurimoto Y. Restoration of the photoreceptor outer segment and visual outcomes after macular hole closure: Spectral-domain optical coherence tomography analysis. Graefe's Archive for Clinical and Experimental Ophthalmology. 2011;**249**(10):1469-1476

[13] Wakabayashi T, Fujiwara M, Sakaguchi H, Kusaka S, Oshima Y. Foveal microstructure and visual acuity in surgically closed macular holes: Spectral-domain optical coherence tomographic analysis. Ophthalmology. 2010;**117**(9):1815-1824

[14] Oishi A, Shimozono M, Mandai M, Hata M, Nishida A, Kurimoto Y. Recovery of photoreceptor outer segments after anti-VEGF therapy for

age-related macular degeneration. Graefe's Archive for Clinical and Experimental Ophthalmology. 2013;**251**(2):435-440

[15] Hartmann KI, Gomez ML, Bartsch D-UG, Schuster AK, Freeman WR. Effect of change in drusen evolution on photoreceptor inner segment/outer segment junction. Retina. 2012;**32**(8):1492-1499

[16] Mrejen S, Sato T, Curcio CA, Spaide RF. Assessing the cone photoreceptor mosaic in eyes with pseudodrusen and soft drusen in vivo using adaptive optics imaging. Ophthalmology. 2014;**121**(2):545-551

[17] Curcio CA, Messinger JD, Sloan KR, McGwin G, Medeiros NE, Spaide RF. Subretinal drusenoid deposits in non-neovascular age-related macular degeneration: Morphology, prevalence, topography, and biogenesis model. Retina. 2013;**33**(2):265-276

[18] Pilotto E, Benetti E, Convento E, Guidolin F, Longhin E, Parrozzani R, et al. Microperimetry, fundus autofluorescence, and retinal layer changes in progressing geographic atrophy. Canadian Journal of Ophthalmology. 2013;**48**(5):386-393

[19] Maheshwary AS, Oster SF, Yuson RMS, Cheng L, Mojana F, Freeman WR. The association between percent disruption of the photoreceptor inner segment-outer segment junction and visual acuity in diabetic macular edema. American Journal of Ophthalmology. 2010;**150**(1):63-67.e1

[20] Jain A, Saxena S, Khanna VK, Shukla RK, Meyer CH. Status of serum VEGF and ICAM-1 and its association with external limiting membrane and inner segment-outer segment junction disruption in type 2 diabetes mellitus. Molecular Vision. 2013;**19**:1760-1768

[21] Itoh Y, Inoue M, Rii T, Hirota K, Hirakata A. Correlation between foveal cone outer segment tips line and visual recovery after epiretinal membrane surgery. Investigative Ophthalmology & Visual Science. 2013;**54**(12):7302

[22] Inoue M, Morita S, Watanabe Y, Kaneko T, Yamane S, Kobayashi S, et al. Inner segment/outer segment junction assessed by spectral-domain optical coherence tomography in patients with idiopathic epiretinal membrane. American Journal of Ophthalmology. 2010;**150**(6):834-839

[23] Suh MH, Seo JM, Park KH, Yu HG. Associations between macular findings by optical coherence tomography and visual outcomes after epiretinal membrane removal. American Journal of Ophthalmology. 2009;**147**(3):473-480.e3

[24] Gharbiya M, Grandinetti F, Scavella V, Cecere M, Esposito M, Segnalini A, et al. Correlation between spectral-domain optical coherence tomography findings and visual outcome after primary rhegmatogenous retinal detachment repair. Retina. 2012;**32**(1):43-53

[25] Coscas G, De Benedetto U, Coscas F, Li Calzi CI, Vismara S, Roudot-Thoraval F, et al. Hyperreflective dots: A new spectral-domain optical coherence tomography entity for follow-up and prognosis in exudative age-related macular degeneration. Ophthalmologica. 2013;**229**(1):32-37

[26] Bolz M, Schmidt-Erfurth U, Deak G, Mylonas G, Kriechbaum K, Scholda C. Optical coherence tomographic hyperreflective foci. Ophthalmology. 2009;**116**(5):914-920

[27] Vujosevic S, Bini S, Midena G, Berton M, Pilotto E, Midena E. Hyperreflective intraretinal spots in diabetics without and with nonproliferative diabetic retinopathy: An in vivo study using spectral domain OCT. Journal Diabetes Research. 2013;**2013**:1-5

[28] Vujosevic S, Torresin T, Bini S, Convento E, Pilotto E, Parrozzani R, et al. Imaging retinal inflammatory biomarkers after intravitreal steroid and anti-VEGF treatment in diabetic macular oedema. Acta Ophthalmologica. 2017;**95**(5):464-471

[29] Coscas G, Loewenstein A, Augustin A, Bandello F, Battaglia Parodi M, Lanzetta P, et al. Management of retinal vein occlusion—Consensus document. Ophthalmologica. 2011;**226**(1):4-28

[30] Ogino K, Murakami T, Tsujikawa A, Miyamoto K, Sakamoto A, Ota M, et al. Characteristics of optical coherence tomographic hyperreflective foci in retinal vein occlusion. Retina. 2012;**32**(1):77-85

[31] Uji A, Murakami T, Nishijima K, Akagi T, Horii T, Arakawa N, et al. Association between hyperreflective foci in the outer retina, status of photoreceptor layer, and visual acuity in diabetic macular edema. American Journal of Ophthalmology. 2012;**153**(4):710-717.e1

[32] Hwang HS, Chae JB, Kim JY, Kim DY. Association between hyperreflective dots on spectral-domain optical coherence tomography in macular edema and response to treatment. Investigative Ophthalmology & Visual Science. 2017;**58**(13):5958

[33] Mavrikakis I, Sfikakis PP, Mavrikakis E, Rougas K, Nikolaou A, Kostopoulos C, et al. The incidence of irreversible retinal toxicity in patients treated with hydroxychloroquine: A reappraisal. Ophthalmology. 2003;**110**(7):1321-1326

[34] Chen E, Brown DM, Benz MS, Fish RH, Wong TP, Kim RY, et al. Spectral domain optical coherence tomography as an effective screening test for hydroxychloroquine retinopathy (the "flying saucer" sign). Clinical Ophthalmology. 2010;**4**:1151-1158

[35] Ascaso FJ, Rodríguez NA, San Miguel R, Huerva V. The "flying saucer" sign on spectral domain optical coherence tomography in chloroquine retinopathy. Arthritis and Rheumatism. 2013;**65**(9):2322-2322

[36] Zweifel SA. Outer retinal tubulation: A novel optical coherence tomography finding. Archives of Ophthalmology. 2009;**127**(12):1596

[37] Iriyama A, Aihara Y, Yanagi Y. Outer retinal tubulation in inherited retinal degenerative disease. Retina. 2013;**33**(7):1462-1465

[38] Goldberg NR, Greenberg JP, Laud K, Tsang S, Freund KB. Outer retinal tubbulation in degeneration retinal disorders. Retina. 2013;**33**(9):1871-1876

[39] Zweifel SA, Imamura Y, Freund KB, Spaide RF. Multimodal fundus imaging of pseudoxanthoma elasticum. Retina. 2011;**31**(3):482-491

[40] Sambricio J, Tejada-Palacios P, Barceló-Mendiguchía A. Choroidal neovascularization, outer retinal tubulation and fundus autofluorescence findings in a patient with enhanced S-cone syndrome. Clinical & Experimental Ophthalmology. 2016;**44**(1):69-71

[41] Schaal KB, Freund KB, Litts KM, Zhang Y, Messinger JD, Curcio CA. Outer retinal tubulation in advanced age-related macular degeneration: Optical coherence tomographic findings correspond to histology. Retina. 2015;**35**(7):1339-1350

[42] Dolz-Marco R, Litts KM, Tan ACS, Freund KB, Curcio CA. The evolution of outer retinal tubulation, a neurodegeneration and gliosis prominent in macular diseases. Ophthalmology. 2017;**124**(9):1353-1367

[43] Caillaux V, Gaucher D, Gualino V, Massin P, Tadayoni R, Gaudric A.

Morphologic characterization of dome-shaped macula in myopic eyes with serous macular detachment. American Journal of Ophthalmology. 2013;**156**(5):958-967.e1

[44] Errera M-H, Michaelides M, Keane PA, Restori M, Paques M, Moore AT, et al. The extended clinical phenotype of dome-shaped macula. Graefe's Archive for Clinical and Experimental Ophthalmology. 2014;**252**(3):499-508

[45] Keane PA, Mitra A, Khan IJ, Quhill F, Elsherbiny SM. Dome-shaped macula: A compensatory mechanism in myopic anisometropia? Ophthalmic Surgery, Lasers & Imaging: The Official Journal of the International Society for Imaging in the Eye. 2012;**43 Online**:e52-e54

[46] Imamura Y, Iida T, Maruko I, Zweifel SA, Spaide RF. Enhanced depth imaging optical coherence tomography of the sclera in dome-shaped macula. American Journal of Ophthalmology. 2011;**151**(2):297-302

[47] Mehdizadeh M, Nowroozzadeh MH. Dome-shaped macula in eyes with myopic posterior staphyloma. American Journal of Ophthalmology. 2008;**146**(3):478-479

[48] Gaucher D, Erginay A, Lecleire-Collet A, Haouchine B, Puech M, Cohen S-Y, et al. Dome-shaped macula in eyes with myopic posterior staphyloma. American Journal of Ophthalmology. 2008;**145**(5):909-914

[49] Ellabban AA, Tsujikawa A, Matsumoto A, Yamashiro K, Oishi A, Ooto S, et al. Three-dimensional tomographic features of dome-shaped macula by swept-source optical coherence tomography. American Journal of Ophthalmology. 2013;**155**(2):320-328.e2

[50] Ohsugi H, Ikuno Y, Oshima K, Yamauchi T, Tabuchi H. Morphologic characteristics of macular complications of a dome-shaped macula determined by swept-source optical coherence tomography. American Journal of Ophthalmology. 2014;**158**(1):162-170.e1

[51] Lorenzo D, Arias L, Choudhry N, Millan E, Flores I, Rubio MJ, et al. Dome-shaped macula in myopic eyes: Twelve-month follow-up. Retina. 2017;**37**(4):680-686

[52] Soudier G, Gaudric A, Gualino V, Massin P, Nardin M, Tadayoni R, et al. Long-term evolution of dome-shaped macula: Increased macular bulge is associated with extended macular atrophy. Retina. 2016;**36**(5):944-952

[53] Daruich A, Matet A, Dirani A, Bousquet E, Zhao M, Farman N, et al. Central serous chorioretinopathy: Recent findings and new physiopathology hypothesis. Progress in Retinal and Eye Research. 2015;**48**:82-118

[54] Matsumoto H, Kishi S, Sato T, Mukai R. Fundus autofluorescence of elongated photoreceptor outer segments in central serous chorioretinopathy. American Journal of Ophthalmology. 2011;**151**(4):617-623.e1

[55] Spaide RF, Klancnik JM. Fundus autofluorescence and central serous chorioretinopathy. Ophthalmology. 2005;**112**(5):825-833

[56] Drexler W, Morgner U, Ghanta RK, Kärtner FX, Schuman JS, Fujimoto JG. Ultrahigh-resolution ophthalmic optical coherence tomography. Nature Medicine. 2001;**7**(4):502-507

[57] Pianta MJ, Aleman TS, Cideciyan AV, Sunness JS, Li Y, Campochiaro BA, et al. In vivo micropathology of best macular dystrophy with optical coherence tomography. Experimental Eye Research. 2003;**76**(2):203-211

[58] Sun JK, Radwan SH, Soliman AZ, Lammer J, Lin MM, Prager SG, et al.

Neural retinal disorganization as a robust marker of visual acuity in current and resolved diabetic macular edema. Diabetes. 2015;**64**(7):2560-2570

[59] Nicholson L, Ramu J, Triantafyllopoulou I, Patrao NV, Comyn O, Hykin P, et al. Diagnostic accuracy of disorganization of the retinal inner layers in detecting macular capillary non-perfusion in diabetic retinopathy. Clinical & Experimental Ophthalmology. 2015;**43**(8):735-741

[60] Moein H-R, Novais EA, Rebhun CB, Cole ED, Louzada RN, Witkin AJ, et al. Optical coherence tomography angiography to detect macular capillary ischemia in patients with inner retinal changes after resolved diabetic macular edema. Retina. 2018;**38**(12):2277-2284

[61] Bek T. Transretinal histopathological changes in capillary-free areas of diabetic retinopathy. Acta Ophthalmologica. 1994; **72**(4):409-415

[62] Barber AJ, Lieth E, Khin SA, Antonetti DA, Buchanan AG, Gardner TW. Neural apoptosis in the retina during experimental and human diabetes. Early onset and effect of insulin. The Journal of Clinical Investigation. 1998;**102**(4):783-791

[63] Grewal DS, O'Sullivan ML, Kron M, Jaffe GJ. Association of disorganization of retinal inner layers with visual acuity in eyes with uveitic cystoid macular edema. American Journal of Ophthalmology. 2017;**177**:116-125

[64] Berry D, Thomas AS, Fekrat S, Grewal DS. Association of disorganization of retinal inner layers with ischemic index and visual acuity in central retinal vein occlusion. Ophthalmology Retina. 2018;**2**(11):1125-1132

[65] Balaratnasingam C, Inoue M, Ahn S, McCann J, Dhrami-Gavazi E, Yannuzzi LA, et al. Visual acuity is correlated with the area of the foveal avascular zone in diabetic retinopathy and retinal vein occlusion. Ophthalmology. 2016;**123**(11):2352-2367

[66] Joltikov KA, Sesi CA, de Castro VM, Davila JR, Anand R, Khan SM, et al. Disorganization of retinal inner layers (DRIL) and neuroretinal dysfunction in early diabetic retinopathy. Investigative Ophthalmology & Visual Science. 2018;**59**(13):5481-5486

[67] Das R, Spence G, Hogg RE, Stevenson M, Chakravarthy U. Disorganization of inner retina and outer retinal morphology in diabetic macular edema. JAMA Ophthalmology. 2018;**136**(2):202-208

[68] Radwan SH, Soliman AZ, Tokarev J, Zhang L, van Kuijk FJ, Koozekanani DD. Association of disorganization of retinal inner layers with vision after resolution of center-involved diabetic macular edema. JAMA Ophthalmology. 2015;**133**(7):820-825

[69] Sun JK, Lin MM, Lammer J, Prager S, Sarangi R, Silva PS, et al. Disorganization of the retinal inner layers as a predictor of visual acuity in eyes with center-involved diabetic macular edema. JAMA Ophthalmology. 2014;**132**(11):1309-1316

[70] Gelman SK, Freund KB, Shah VP, Sarraf D. The pearl necklace sign: A novel spectral domain optical coherence tomography finding in exudative macular disease. Retina. 2014;**34**(10):2088-2095

[71] Ajay K, Mason F, Gonglore B, Bhatnagar A. Pearl necklace sign in diabetic macular edema: Evaluation and significance. Indian Journal of Ophthalmology. 2016;**64**(11):829-834

[72] Liu G-H, Lin B, Sun X-Q, He Z-F, Li J-R, Zhou R, et al. Focal choroidal excavation: A preliminary interpretation based on clinic and review. International

Journal of Ophthalmology. 2015;**8**(3):513-521

[73] Lee CS, Woo SJ, Kim Y-K, Hwang DJ, Kang HM, Kim H, et al. Clinical and spectral-domain optical coherence tomography findings in patients with focal choroidal excavation. Ophthalmology. 2014;**121**(5):1029-1035

[74] Chung CY, Li SH, Li KKW. Focal choroidal excavation-morphological features and clinical correlation. Eye. 2017;**31**(9):1373-1379

[75] Shinojima A, Kawamura A, Mori R, Yuzawa M. Morphologic features of focal choroidal excavation on spectral domain optical coherence tomography with simultaneous angiography. Retina. 2014;**34**(7):1407-1414

[76] Hashimoto Y, Saito W, Noda K, Ishida S. Acquired focal choroidal excavation associated with multiple evanescent white dot syndrome: Observations at onset and a pathogenic hypothesis. BMC Ophthalmology. 2014;**14**(1):135

[77] Liu W, Gao M, Liang X. Management of subfoveal perfluorocarbon liquid: A review. Ophthalmologica. 2018;**240**(1):1-7

[78] Garcia-Valenzuela E, Ito Y, Abrams GW. Risk factors for retention of subretinal perfluorocarbon liquid in vitreoretinal surgery. Retina. 2004;**24**(5):746-752

[79] Cohen SY, Dubois L, Elmaleh C. Retinal hole as a complication of long-standing subretinal perfluorocarbon liquid. Retina. 2006;**26**(7):843-844

[80] Roth DB, Sears JE, Lewis H. Removal of retained subfoveal perfluoro-n-octane liquid. American Journal of Ophthalmology. 2004;**138**(2):287-289

[81] Lima LH, Laud K, Chang LK, Yannuzzi LA. Choroidal macrovessel. The British Journal of Ophthalmology. 2011;**95**(9):1333-1334

[82] Ehlers JP, Rayess H, Spaide RF. Isolated choroidal macrovessel: A tracklike choroidal lesion. Canadian Journal of Ophthalmology. 2014;**49**(6):e158-e160

[83] Choudhry N, Rao RC. Enhanced depth imaging features of a choroidal macrovessel. Retinal Cases and Brief Reports. 2016;**10**(1):18-21

[84] Kim HC, Cho WB, Chung H. Morphologic changes in acute central serous chorioretinopathy using spectral domain optical coherence tomography. Korean Journal of Ophthalmology. 2012;**26**(5):347-354

[85] Fujimoto H, Gomi F, Wakabayashi T, Sawa M, Tsujikawa M, Tano Y. Morphologic changes in acute central serous chorioretinopathy evaluated by Fourier-domain optical coherence tomography. Ophthalmology. 2008;**115**(9):1494-1500.e2

[86] Thaisiam P, Rattanaumpawan P. Rare manifestations of Streptococcus pneumoniae infection; the first case report in Thailand and literature review of pneumococcal endophthalmitis and endocarditis. Journal of the Medical Association of Thailand. 2014;**97**(12):1364-1369